Journal of Sound and Vibration (1998) **210**(1), 69–89

HIGHER ORDER TIME-STEP INTEGRATION METHODS WITH COMPLEX TIME STEPS

T. C. FUNG

School of Civil and Structural Engineering, Nanyang Technological University, Nanyang Avenue, Singapore 639798

(*Received* 23 *January* 1997, *and in final form* 28 *August* 1997)

Unconditionally stable higher order time-step integration algorithms are presented. The algorithms are based on the Newmark method with complex time steps. The numerical results at the (complex) sub-step locations are combined linearly to give higher order accurate results at the end of the time step. The ultimate spectral radius in the high-frequency range is a controllable parameter for these algorithms. Among these algorithms, the asymptotic annihilating algorithm and the non-dissipative algorithm correspond to the first sub-diagonal and diagonal Padé approximations respectively. The characteristics of the present algorithms with various numerical dissipations are found to be in between these two algorithms. The algorithmic parameters for the third, fifth and seventh order algorithms with various numerical dissipations are given explicitly. The order of accuracy is increased by one if these algorithms are set to non-dissipative. The spectral radii, algorithm damping ratios and relative period errors are compared favourably with other higher order algorithms.

1. INTRODUCTION

It is common to obtain the numerical solutions for structural dynamic problems using step-by-step time integration algorithms. There are advantages for the algorithms to possess numerical dissipation so as to damp out the spurious high-frequency responses. Wood [1] suggested that the curve of the spectral radius against $\Delta t/T$ (where T is the undamped natural period and Δt is the time step) should stay close to unit level as long as possible and decrease to about 0·5–0·8 as $\Delta t/T$ tends to infinity. The corresponding spectral radius as $\Delta t/T \to \infty$ is defined as the ultimate spectral radius and is denoted by μ in this paper. In the extreme case, the ulitimate spectral radius approaches zero so that the high-frequency responses are eliminated in one time step. The algorithms with this property are asymptotic annihilating.

Apart from numerical dissipation, the algorithms should be unconditionally stable so that time steps of any size can be used without introducing numerical instability. The ability in using a large time step is of advantage to structural dynamic problems where the responses are contributed to mainly by the low-frequency modes. The time-step sizes need not be too small to resolve the very high frequency modes accurately, as long as the algorithm remains numerically stable.

The Newmark method is the most widely used algorithm for structural dynamic problems. However, the algorithm is only first order accurate when it is dissipative. The second order accurate Newmark method is non-dissipative.

There are other algorithms that are unconditionally stable, second order accurate and possess numerical dissipation, e.g., Wilson-θ method, collocation method, Houbolt

0022–460X/98/060069 + 21 $25.00/0/sv971300

method, Park method, HHT-α method and Generalized-α method. A more detailed description of these algorithms can be found in books by Wood [1], Hughes [2] and Zienkiewicz and Taylor [3].

Higher order accurate algorithms that are unconditionally stable and non-dissipative can be constructed from the diagonal Padé approximations [4, 5], Runge–Kutta methods [4, 5], weighted residual methods [1, 3], Petrov–Galerkin method [6] or bi-discontinuous time Galerkin method [7].

Higher order accurate algorithms that are unconditionally stable and asymptotic annihilating can be constructed from the discontinuous Galerkin method [7, 8, 9], Petrov–Galerkin method [6] and weighted residual methods [10].

Other higher order accurate dissipative algorithms can be obtained from Runge–Kutta methods [4, 5], bi-discontinuous time Galerkin method [7] and weighted residual methods [1, 3]. However, the high-frequency dissipation is not a directly controllable parameter in these algorithms. Sometimes, there are cusps in the curves of the spectral radii against $\Delta t/T$ for the algorithms. It is undesirable as the responses in the mid-frequency range would have more algorithmic damping than those in the high-frequency range.

Higher order algorithms can also be constructed by using the Romberg extrapolation technique [11]. The accuracy of the solutions obtained from the second order accurate Newmark method is improved by evaluating the results at the end of the time step a few times with different sub-step sizes. The fourth, sixth and eighth order algorithms can be constructed with 3, 7 and 15 evaluations. The numerical results are very accurate and are comparable to the Padé approximations. However, these extrapolated Newmark methods are unconditionally unstable, i.e., the spectral radius is greater than unity even for very small time steps. Very small time-step sizes are required to maintain numerical stability.

Recently, Zhong and Williams [12] proposed a precise time-step integration method. The second order differential equations were transformed into an equivalent first order form. The exact homogeneous solution is expressed in terms of the exponent of the coefficient matrix. The special feature of the method was that the exponential matrix was evaluated recursively from a truncated Taylor's series approximation. The number of recursive evaluations was set to 20 and a highly precise time-step integration algorithm was obtained. The exponential matrix so obtained can be regarded as numerically exact. Solution algorithms for various non-linearly varying excitations were given explicitly [13].

The computational effort, however, is very high as many matrix multiplications are required. The method is found to be suitable for structural non-stationary random response problems and problems formulated by the boundary element method, where the matrices are fully populated [12]. The method can also be used to generate convincing benchmark solutions [12]. The computation efficiency can be improved by using the sub-domain method [14] or the step-response and impulsive-response matrices [15].

1.1. TARNOW AND SIMO'S SUB-MARCHING PROCEDURE

Recently, Tarnow and Simo [16] presented a sub-marching procedure (Figure 1(a)) to construct fourth order accurate algorithms from a fairly general class of second order accurate algorithms. In their procedure, a sequential sub-marching (forward and backward) of three evaluations is required to advance one time step. The stability, conservative properties and implementation of the underlying second order algorithm are retained. When the procedure is applied to the second order Newmark method, the resultant algorithm is non-dissipative. To introduce high-frequency dissipation, the post-process filtering of the solution is suggested.

In this paper, a sub-stepping procedure (Figure 1(b)) is proposed. The numerical results at different sub-step locations are evaluated independently and then combined linearly to

give higher order accurate results at the end of the time step. As in Tarnow and Simo's procedure, there are no changes in the implementation of the underlying Newmark method except the use of complex time steps. However, the high-frequency dissipation is controllable for the present algorithms. Besides, as the numerical results at the sub-step locations are independent of each other, the evaluations can be computed in parallel. Furthermore, the present procedure is more general as it can construct other higher order algorithms systematically from the underlying second order accurate Newmark algorithm.

1.2. OUTLINE OF THE PAPER

Unconditionally stable higher order accurate step-by-step time integration algorithms with controllable numerical dissipation are constructed. The Newmark method with complex time steps is used. The numerical results at the end of a time step are obtained by combining results at several sub-step locations. The weighting factors and the sub-step locations are algorithmic parameters. As shown in sections 5 and 6, the algorithmic parameters are chosen to eliminate the leading trucation error terms and to give the desirable ultimate spectral radius μ.

It is shown that for $1 \geqslant \mu > -1$, the algorithms are unconditionally stable. The spectral radius decreases progressively to the required ultimate spectral radius μ as $\Delta t/T$ increases. The high-frequency responses are subjected to more algorithmic damping as required. Besides, the eigenvalues for the numerical amplification matrix are complex conjugates. As a result, the algorithms derived are unconditionally C-stable and higher order accurate.

The third order algorithms are derived in detail in section 7. The algorithmic parameters for the fifth and seventh order algorithms are given explicitly in section 8. The present asymptotic annihilating algorithm ($\mu = 0$) and non-dissipative algorithm ($\mu = 1$) are found to be the first sub-diagonal and diagonal Padé approximations respectively. Hence, for the present non-dissipative algorithms, the order of accuracy is increased by one.

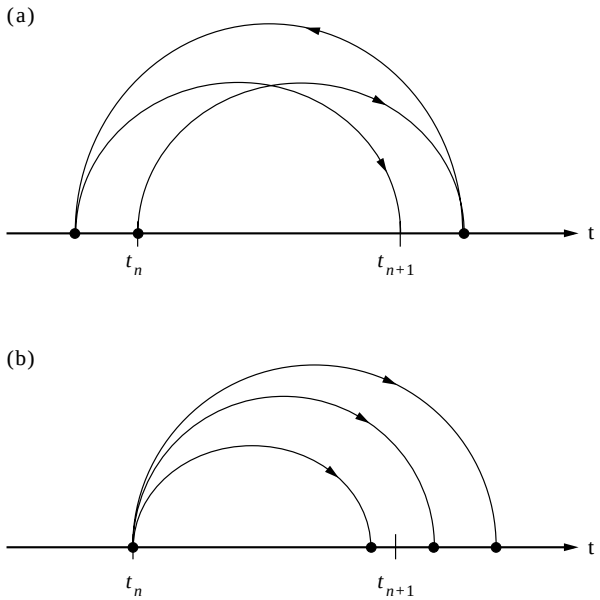

Figure 1. Sub-marching (a) and sub-stepping (b) procedures. ●, Results to be used to find the response at t_{n+1}.

In section 9, the spectral radii, the algorithmic damping ratios and the relative period errors of the present proposed higher order algorithms are compared with other higher order algorithms. A numerical example is given in section 10 to illustrate the present higher order accurate algorithms.

2. EQUATIONS OF MOTION

The equations of motion of a multi-degree-of-freedom system after spatial discretization using the finite element method can be written as

$$[\mathbf{M}]\{\ddot{\mathbf{u}}(t)\} + [\mathbf{C}]\{\dot{\mathbf{u}}(t)\} + [\mathbf{K}]\{\mathbf{u}(t)\} = \{\mathbf{F}(t)\}, \tag{1}$$

where [**M**], [**C**] and [**K**] are the mass, damping and stiffness matrices respectively, $\{\mathbf{F}(t)\}$ is the applied load vector, $\{\mathbf{u}(t)\}$ is the unknown displacement vector which in general is a function of time t and dots denote differentiation with respect to time t. The initial conditions at $t = 0$ are $\{\mathbf{u}(0)\} = \{\mathbf{u}_0\}$ and $\{\dot{\mathbf{u}}(0)\} = \{\mathbf{v}_0\}$. The numerical solutions of equation (1) can be obtained by step-by-step time integration methods.

It would be cumbersome and difficult to study the characteristics of an algorithm by applying it to equation (1) directly. Instead, the modal decomposition method can be used to uncouple equation (1) by involving the orthogonality properties of the free vibration mode shapes of the undamped system. In this case, modal damping is assumed.

It has been rigorously established that the integration of the uncoupled equations is equivalent to the integration of the original system [1–4]. It is therefore more convenient and sufficient for the purpose of investigating the characteristics of a proposed algorithm to consider the equation of motion of a single-degree-of-freedom system in the form

$$\ddot{u}(t) + 2\xi\omega\dot{u}(t) + \omega^2 u(t) = f(t), \tag{2}$$

where ξ, ω and $f(t)$ are the damping ratio, undamped natural frequency of the system and the forcing excitation respectively.

3. NEWMARK METHOD

Equation (1) can be solved by the Newmark method. The numerical solutions $\{\mathbf{u}_{n+1}\}$ and $\{\mathbf{v}_{n+1}\}$ approximating $\{\mathbf{u}(t)\}$ and $\{\dot{\mathbf{u}}(t)\}$ respectively at $t = t_{n+1}$ can be obtained from $\{\mathbf{u}_n\}$ and $\{\mathbf{v}_n\}$ at $t = t_n$ by

$$\{\mathbf{u}_{n+1}\} = \{\mathbf{u}_n\} + \Delta t\{\mathbf{v}_n\} + \Delta t^2(1 - 2\beta)/2\{\mathbf{a}_n\} + \Delta t^2\beta\{\mathbf{a}_{n+1}\}, \tag{3a}$$

$$\{\mathbf{v}_{n+1}\} = \{\mathbf{v}_n\} + \Delta t(1 - \gamma)\{\mathbf{a}_n\} + \Delta t\gamma\{\mathbf{a}_{n+1}\}, \tag{3b}$$

$$[\mathbf{M}]\{\mathbf{a}_n\} + [\mathbf{C}]\{\mathbf{v}_n\} + [\mathbf{K}]\{\mathbf{u}_n\} = \{\mathbf{F}(t_n)\}, \tag{3c}$$

$$[\mathbf{M}]\{\mathbf{a}_{n+1}\} + [\mathbf{C}]\{\mathbf{v}_{n+1}\} + [\mathbf{K}]\{\mathbf{u}_{n+1}\} = \{\mathbf{F}(t_{n+1})\}, \tag{3d}$$

where $\Delta t = t_{n+1} - t_n$, β and γ are the algorithmic parameters. Starting from the given initial conditions $\{\mathbf{u}_0\}$ and $\{\mathbf{v}_0\}$ at $t = 0$, the approximate numerical solutions at other time point $t = t_n$ can be found by using equations (3a–d) repeatedly. To analyse a time-step integration algorithm, t_n and t_{n+1} can be conveniently chosen as 0 and Δt respectively.

3.1. SINGLE-DEGREE-OF-FREEDOM SYSTEM

Equation (2) is used to study the characteristics of the Newmark algorithm and the constructed higher order algorithms. There are many ways to express the Newmark algorithm. Equation (3) is the single-step three-stage form. For comparison with the

analytical solutions, the Newmark algorithm is cast in the equivalent single-step two-stage form for the single-degree-of-freedom system as

$$\begin{Bmatrix} u_{n+1} \\ v_{n+1} \end{Bmatrix} = [\mathbf{A}_{NM}(\Delta t)] \begin{Bmatrix} u_n \\ v_n \end{Bmatrix} + [\mathbf{L}_{NM}(\Delta t)] \begin{Bmatrix} f(t_n) \\ f(t_{n+1}) \end{Bmatrix}, \tag{4}$$

where $[\mathbf{A}_{NM}(\Delta t)]$ is the numerical amplification matrix and is given by

$$\begin{bmatrix} \dfrac{2(2\beta-\gamma)\xi\omega^3\Delta t^3+(2\beta-1)\omega^2\Delta t^2 \\ +4\gamma\xi\omega\Delta t+2}{2+4\gamma\xi\omega\Delta t+2\beta\omega^2\Delta t^2} & 2\dfrac{2(2\beta-\gamma)\xi^2\omega^2\Delta t^3+(2\gamma-1)\xi\omega\Delta t^2+\Delta t}{2+4\gamma\xi\omega\Delta t+2\beta\omega^2\Delta t^2} \\ \dfrac{-(2\beta-\gamma)\omega^4\Delta t^3-2\omega^2\Delta t}{2+4\gamma\xi\omega\Delta t+2\beta\omega^2\Delta t^2} & 2\dfrac{-(2\beta-\gamma)\xi\omega^3\Delta t^3+(\beta-\gamma)\omega^2\Delta t^2+2(\gamma-1)\xi\omega\Delta t+1}{2+4\gamma\xi\omega\Delta t+2\beta\omega^2\Delta t^2} \end{bmatrix}$$

and

$$[\mathbf{L}_{NM}(\Delta t)] = \begin{bmatrix} \dfrac{(1-2\beta)\Delta t^2+2\xi(\gamma-2\beta)\omega\Delta t^3}{2+4\gamma\xi\omega\Delta t+2\beta\omega^2\Delta t^2} & \dfrac{2\beta\Delta t^2}{2+4\gamma\xi\omega\Delta t+2\beta\omega^2\Delta t^2} \\ \dfrac{2(1-\gamma)\Delta t-(\gamma-2\beta)\omega^2\Delta t^3}{2+4\gamma\xi\omega\Delta t+2\beta\omega^2\Delta t^2} & \dfrac{2\gamma\Delta t}{2+4\gamma\xi\omega\Delta t+2\beta\omega^2\Delta t^2} \end{bmatrix}.$$

The Taylor series expansions of the entries in $[\mathbf{A}_{NM}(\Delta t)]$ about $\Delta t = 0$ are useful when studying the truncation errors. They are given by

$$\mathbf{A}_{NM}(1,1) = 1 - \tfrac{1}{2}\omega^2\Delta t^2 + 2\beta\xi\omega^3\Delta t^3 - \tfrac{1}{2}\beta(8\gamma\xi^2-1)\omega^4\Delta t^4 - \beta\xi(2\beta+\gamma-8\gamma^2\xi^2)\omega^5\Delta t^5 + \cdots, \tag{5a}$$

$$\mathbf{A}_{NM}(1,2) = \Delta t - \xi\omega\Delta t^2 + \beta(4\xi^2-1)\omega^2\Delta t^3 - \beta\xi(2\gamma(4\xi^2-1)-1)\omega^3\Delta t^4 - \beta(2\gamma\xi^2+(\beta-4\gamma^2\xi^2)(4\xi^2-1))\omega^4\Delta t^5 + \cdots, \tag{5b}$$

$$\mathbf{A}_{NM}(2,1) = -\omega^2\Delta t + 2\gamma\xi\omega^3\Delta t^2 - \tfrac{1}{2}\gamma(8\gamma\xi^2-1)\omega^4\Delta t^3 - (-8\gamma^2\xi^2+\gamma+2\beta) \times \gamma\xi\omega^5\Delta t^4 - \tfrac{1}{2}\gamma(4\gamma^2\xi^2(1-8\gamma\xi^2)+ \quad 16\beta\gamma\xi^2-\beta)\omega^6\Delta t^5 + \cdots, \tag{5c}$$

$$\mathbf{A}_{NM}(2,2) = 1 - 2\xi\omega\Delta t + \gamma(4\xi^2-1)\omega^2\Delta t^2 - \gamma\xi(2\gamma(4\xi^2-1)-1)\omega^3\Delta t^3 - \gamma(4\gamma^2\xi^2(1-4\xi^2)+2(\gamma+2\beta)\xi^2-\beta)\omega^4\Delta t^4 + \gamma\xi(8\gamma^3\xi^2(1-4\xi^2)+4\gamma(\gamma+4\beta)\xi^2-\beta(1+4\gamma))\omega^5\Delta t^5 + \cdots. \tag{5d}$$

4. TRUNCATION ERRORS

The convergence of a numerical algorithm requires consistency and stability according to Lax equivalent theorem. The consistency property can be determined from the truncation error by comparing the numerical amplification matrix with the analytical amplification matrix. The stability requirements and other measures of accuracy would be considered in the next few sections.

The analytical amplification matrix for equation (2) is given by

$$[\mathbf{A}(\Delta t)] = \mathrm{e}^{-\xi\omega\Delta t} \begin{bmatrix} \cos(\omega_d\Delta t) + \dfrac{\xi\omega}{\omega_d}\sin(\omega_d\Delta t) & \dfrac{1}{\omega_d}\sin(\omega_d\Delta t) \\ -\dfrac{\omega^2}{\omega_d}\sin(\omega_d\Delta t) & \cos(\omega_d\Delta t) - \dfrac{\xi\omega}{\omega_d}\sin(\omega_d\Delta t) \end{bmatrix}, \tag{6}$$

where $\omega_d = \sqrt{1-\xi^2}\omega$ is the damped vibration frequency.

The Taylor series expansions of the entries in [**A**] about $\Delta t = 0$ are

$$\mathbf{A}(1,1) = 1 - \tfrac{1}{2}\omega^2\Delta t^2 + \tfrac{1}{3}\xi\omega^3\Delta t^3 - \tfrac{1}{24}(4\xi^2 - 1)\omega^4\Delta t^4 + \tfrac{1}{30}\xi(2\xi^2 - 1)\omega^5\Delta t^5 + \cdots, \quad (7a)$$

$$\mathbf{A}(1,2) = \Delta t - \xi\omega\Delta t^2 + \tfrac{1}{6}(4\xi^2 - 1)\omega^2\Delta t^3 - \tfrac{1}{6}\xi(2\xi^2 - 1)\omega^3\Delta t^4 + \tfrac{1}{120}(16\xi^4 - 12\xi^2 + 1)\omega^4\Delta t^5 + \cdots, \quad (7b)$$

$$\mathbf{A}(2,1) = -\omega^2\Delta t + \xi\omega^3\Delta t^2 - \tfrac{1}{6}(4\xi^2 - 1)\omega^4\Delta t^3 + \tfrac{1}{6}\xi(2\xi^2 - 1)\omega^5\Delta t^4 - \tfrac{1}{120}(16\xi^4 - 12\xi^2 + 1)\omega^6\Delta t^5 + \cdots, \quad (7c)$$

$$\mathbf{A}(2,2) = 1 - 2\xi\omega\Delta t + \tfrac{1}{2}(4\xi^2 - 1)\omega^2\Delta t^2 - \tfrac{2}{3}\xi(2\xi^2 - 1)\omega^3\Delta t^3 + \tfrac{1}{24}(16\xi^4 - 12\xi^2 + 1)\omega^4\Delta t^4 - \tfrac{1}{60}\xi(16\xi^4 - 16\xi^2 + 3)\omega^5\Delta t^5 + \cdots. \quad (7d)$$

Comparing equations (5) and (7), it can be seen that the truncation errors are $O(\Delta t^3)$ (i.e., second order accurate) if $\gamma = 1/2$ and $O(\Delta t^2)$ (i.e., first order accurate) otherwise. The leading truncation errors can be eliminated by linearly combining the numerical amplification matrices at various sub-step locations ($\beta_i\,\Delta t$) with weighting factor α_i as shown in the next section.

5. TRUNCATION ERROR ELIMINATION PROCEDURE

The sth order accurate numerical amplification matrix [$\mathbf{A}_s\,(\Delta t)$] with truncation error $O(\Delta t^{s+1})$ is to be constructed from

$$[\mathbf{A}_s\,(\Delta t)] = \Sigma\alpha_i\,[\mathbf{A}_{NM}\,(\beta_i\,\Delta t)], \quad (8)$$

where α_i and β_i are algorithmic parameters to be determined. The range of the index i depends on the number of parameters used and is not specified at the mean time. The algorithmic parameters are chosen so that the Taylor series expansions of equations (7) and (8) match for the first $(s+1)$ terms, i.e., from Δt^0 to Δt^s.

Comparing the Taylor series expansions of the entries in [$\mathbf{A}_s$] with those in [**A**], it can be shown that the conditions to match the sth terms are as follows:

$$\text{for } s = 0, \quad \Sigma\alpha_i = 1, \quad (9a)$$

$$\text{for } s = 1, \quad \Sigma\alpha_i\,\beta_i = 1, \quad (9b)$$

$$\text{for } s = 2, \quad \Sigma\alpha_i\,\beta_i^2 = 1, \quad \text{and} \quad \gamma = 1/2, \quad (9c)$$

$$\text{for } s = 3, \quad \Sigma\alpha_i\,\beta_i^3 = 2/3, \quad \text{and} \quad \beta = 1/4, \quad (9d)$$

$$\text{for } s = 4, \quad \Sigma\alpha_i\,\beta_i^4 = 1/3, \quad (9e)$$

$$\text{for } s = 5, \quad \Sigma\alpha_i\,\beta_i^5 = 2/15, \quad (9f)$$

$$\text{or in general, for } s = n, \quad \Sigma\alpha_i\,\beta_i^n = 2^{n-1}/n! \quad (9g)$$

For example, to obtain a second order algorithm, $\gamma = 1/2$ and α_i and β_i must satisfy equations (9a–c). It can be done easily by choosing $\alpha_1 = 1$ and $\beta_1 = 1$. This is of course the original Newmark algorithm. Higher order algorithms can be constructed systematically by solving more equations with more undetermined algorithmic parameters.

It can be seen that for $\beta_0 = 0$, $[\mathbf{A}_{NM}(0)] = [\mathbf{I}]$ is an identity matrix. No evaluation is required. Therefore, it is at no cost to assume one of the sub-step locations to be at the beginning of the time interval, i.e., $\beta_0 = 0$. The corresponding weighting factor α_0 will be determined with other algorithmic parameters when constructing higher order algorithms.

6. HIGH-FREQUENCY NUMERICAL DISSIPATION

The spectral radius is defined as the largest magnitude of the eigenvalues of a numerical amplification matrix. It is a function of $\omega\Delta t$ (or $\Delta t/T$) and other algorithmic parameters. For unconditionally stable algorithms, the spectral radius must be less than unity for all $\omega\Delta t$. In the following, the spectral radius as $\Delta t/T$ (or Δt if T is considered fixed) approaching infinity is considered.

For third or higher order algorithms, as in equation (9), it is required that $\beta = 1/4$ and $\gamma = 1/2$. The numerical amplification matrix in equation (8) as Δt approaches infinity is given by

$$\lim_{\Delta t\to\infty}[\mathbf{A}_s(\Delta t)] = \lim_{\Delta t\to\infty}\Sigma\alpha_i[\mathbf{A}_{NM}(\beta_i\,\Delta t)] = \alpha_0\begin{bmatrix}1 & 0\\ 0 & 1\end{bmatrix} + \sum_{i\neq 0}\alpha_i\begin{bmatrix}-1 & 0\\ 0 & -1\end{bmatrix}. \tag{10}$$

The magnitude of the eigenvalues $|\lambda_\infty|$ is the square root of the determinant of the matrix in equation (10). Let μ denote this ultimate spectral radius, then

$$\mu^2 = \det\left(\lim_{\Delta t\to\infty}[\mathbf{A}_s(\Delta t)]\right) = \left(\alpha_0 - \sum_{i\neq 0}\alpha_i\right)^2 = (2\alpha_0 - 1)^2, \tag{11}$$

by using equation (9a). Hence the weighting factor α_0 for the initial condition is related to the ultimate spectral radius, i.e.,

$$\alpha_0 = \tfrac{1}{2}(1 \pm \mu). \tag{12}$$

The sign of μ is chosen so that the algorithm is undefined as $\mu = -1$ as shown in the following sections.

7. THIRD ORDER COMPLEX-TIME-STEP ALGORITHMS

Using three pairs of α_i and β_i and assuming $\beta_0 = 0$, there are five unknowns α_0, α_1, α_2, β_1 and β_2 to be determined. They can be used to solve five equations, in particular, equations (9a–d) and (12). The resultant algorithm is at least third order accurate. It can be shown that α_0, α_1, α_2, β_1 and β_2 can be solved in terms of μ as

$$\alpha_0 = \tfrac{1}{2}(1+\mu), \qquad \alpha_1 = \frac{1-\mu}{4} + i\frac{4+7\mu+\mu^2}{4\sqrt{2+2\mu-\mu^2}}, \qquad \alpha_2 = \frac{1-\mu}{4} - i\frac{4+7\mu+\mu^2}{4\sqrt{2+2\mu-\mu^2}}, \tag{13a}$$

$$\beta_0 = 0, \qquad \beta_1 = \frac{2+\mu}{3(1+\mu)} - i\frac{\sqrt{2+2\mu-\mu^2}}{3(1+\mu)}\,\beta_2 = \frac{2+\mu}{3(1+\mu)} + i\frac{\sqrt{2+2\mu-\mu^2}}{3(1+\mu)}, \tag{13b}$$

where $i = \sqrt{-1}$. It can be shown that β_1 and β_2 are the roots of the quadratic equation $3(1+\mu)x^2 - (4+2\mu)x + 2 = 0$. The algorithmic parameters are complex if $1 - \sqrt{3} < \mu < 1 + \sqrt{3}$. Obviously, α_1 and α_2 (β_1 and β_2) are complex conjugate pairs.

The third order numerical amplification matrix $[\mathbf{A}_3(\Delta t)]$ can be written as

$$[\mathbf{A}_3(\Delta t)] = \alpha_0[\mathbf{I}] + \alpha_1[\mathbf{A}_{NM}(\beta_1\Delta t)] + \alpha_2[\mathbf{A}_{NM}(\beta_2\Delta t)]$$
$$= \alpha_0[\mathbf{I}] + \alpha_1[\mathbf{A}_{NM}(\beta_1\Delta t)] + \overline{\alpha_1[\mathbf{A}_{NM}(\beta_1\Delta t)]}, \tag{14}$$

where $\bar{Z}$ is the complex conjugate of Z. It can be seen that even though complex numbers are used, the resultant numerical amplification matrix in equation (14) is real.

It can be shown that the eigenvalues of the undamped numerical amplification matrix (i.e., with $\xi = 0$) are complex conjugates and the squares of the moduli of the eigenvalues are

$$|\lambda_1|^2 = |\lambda_2|^2 = \det([\mathbf{A}_3]) = 1 - \frac{\omega^4\Delta t^4(1-\mu^2)}{\omega^4\Delta t^4 + 4(1+\mu+\mu^2)\omega^2\Delta t^2 + 36(1+\mu)^2}. \tag{15}$$

It can be shown that $\det([\mathbf{A}_3]) \geqslant 0$ for all real values of $\omega\Delta t$ and μ. Also, the algorithm is conditionally stable with the spectral radius exceeding unity for some values of $\omega\Delta t$ if $\mu > 1$ or $\mu < -1$. When μ approaches -1, β_1 and β_2 in equation (13) approach infinity and the formulation is not valid. As a result, the algorithm is unconditionally C-stable only when $1 \geqslant \mu > -1$. Besides, it can be seen that the spectral radius decreases monotonically as $\omega\Delta t$ increases. This gives good algorithmic damping properties as the high-frequency responses are damped out progressively.

The leading truncation error terms for the entries in $[\mathbf{A}_s] - [\mathbf{A}]$ can be shown to be proportional to equation (9e) and are given by

$$\Sigma\alpha_1\beta_1^4 - 1/3 = -\frac{(1-\mu)}{9(1+\mu)}. \tag{16}$$

The errors of an algorithm can be measured by the algorithmic damping ratio and the relative period error. They are related to the numerical dissipation and dispersion (or the amplitude and phase errors). If the complex eigenvalues λ_1 and λ_2 of the numerical amplification matrix are expressed in the following form

$$\lambda_{1,2} = \exp(\bar{\omega}\Delta t(-\bar{\xi} \pm i)), \tag{17}$$

where $i = \sqrt{-1}$, then $\bar{\omega}$ and $\bar{\xi}$ are defined as the algorithmic frequency and algorithmic damping ratio respectively. The relative period error is defined as $(\bar{T} - T)/T$ where $T = 2\pi/\omega$ and $\bar{T} = 2\pi/\bar{\omega}$.

It can be shown that the relative period error and algorithmic damping ratio for the third order accurate algorithm are

$$\text{Relative period error} = \frac{2-\mu+2\mu^2}{540(1+\mu)^2}\omega^4\Delta t^4 + O(\Delta t^6), \tag{18a}$$

$$\text{Algorithmic damping ratio} = \frac{1-\mu}{72(1+\mu)}\omega^3\Delta t^3 + O(\Delta t^5). \tag{18b}$$

From equation (18a), it can be seen that no real value of μ could eliminate the leading error term further. However, the leading error term is minimized if $\mu = 1$. In this case, both equations (16) and (18b) become zero and equation (15) becomes 1. The algorithm is then fourth order accurate and non-dissipative. Besides, it can be seen that if $\mu = -1$, the formulation is not valid as some of the algorithmic parameters are undefined in equation (13).

As $\omega\Delta t$ approaches infinity, it can be shown that the squares of the moduli of the eigenvalues are, as expected,

$$\lim_{\Delta t\to\infty}|\lambda_1|^2 = \lim_{\Delta t\to\infty}|\lambda_2|^2 = |\lambda_\infty|^2 = \mu^2. \tag{19}$$

Hence, for a desirable $|\lambda_\infty|$, two values of μ ($= \pm|\lambda_\infty|$) are possible. However, it can be seen that the errors increase as μ decreases from 1. As a result, for a desirable ultimate spectral radius $|\lambda_\infty|$, $\mu = |\lambda_\infty|$ would give better results than $\mu = -|\lambda_\infty|$. In conclusion, only algorithms with $0 \leqslant \mu \leqslant 1$ would be useful.

For record purposes, the entries in equation (14) can be explicitly written as

$$\mathbf{A}_3(1,1) = \frac{\mu\rho^4 - 4(2\mu+1)\xi\rho^3 - 2(7\mu^2+16\mu+7-12(\mu+1)\xi^2)\rho^2 + 24(\mu+1)(\mu+2)\xi\rho + 36(1+\mu)^2}{\rho^4 + 4(\mu+2)\xi\rho^3 + 4(\mu^2+\mu+1+6(\mu+1)\xi^2)\rho^2 + 24(\mu+1)(\mu+2)\xi\rho + 36(1+\mu)^2}, \tag{20a}$$

$$\mathbf{A}_3(1,2) = \frac{-(2(\mu^2+4\mu+1)\rho^2 + 12(\mu-1)(\mu+1)\xi\rho - 36(1+\mu)^2)\rho/\omega}{\rho^4 + 4(\mu+2)\xi\rho^3 + 4(\mu^2+\mu+1+6(\mu+1)\xi^2)\rho^2 + 24(\mu+1)(\mu+2)\xi\rho + 36(1+\mu)^2}, \tag{20b}$$

$$\mathbf{A}_3(2,1) = \frac{(2(\mu^2+4\mu+1)\rho^2 + 12(\mu-1)(\mu+1)\xi\rho - 36(1+\mu)^2)\rho\omega}{\rho^4 + 4(\mu+2)\xi\rho^3 + 4(\mu^2+\mu+1+(6\mu+1)\xi^2)\rho^2 + 24(\mu+1)(\mu+2)\xi\rho + 36(1+\mu)^2}, \tag{20c}$$

$$\mathbf{A}_3(2,2) = \frac{\mu\rho^4 + 4\mu(\mu+2)\xi\rho^3 - 2(7\mu^2+16\mu+7-12\mu(\mu+1)\xi^2)\rho^2 - 24(\mu+1)(2\mu+1)\xi\rho + 36(1+\mu)^2}{\rho^4 + 4(\mu+2)\xi\rho^3 + 4(\mu^2+\mu+1+6(\mu+1)\xi^2)\rho^2 + 24(\mu+1)(\mu+2)\xi\rho + 36(1+\mu)^2}, \tag{20d}$$

where $\rho = \omega\Delta t$.

7.1. THIRD ORDER ASYMPTOTIC ANNIHILATING ALGORITHM

Consider the asymptotic annihilating algorithm with $\mu = 0$. The algorithmic parameters in equation (13) are

$$\alpha_0 = \frac{1}{2}, \quad \alpha_1 + \frac{1}{4} + i\frac{1}{\sqrt{2}}, \quad \alpha_2 = \frac{1}{4} - i\frac{1}{\sqrt{2}}, \quad \beta_0 = 0, \quad \beta_1 = \frac{2}{3} - i\frac{\sqrt{2}}{3}, \quad \beta_2 = \frac{2}{3} + i\frac{\sqrt{2}}{3}, \tag{21}$$

and the entries of the numerical amplification in equations (20a–d) are

$$\mathbf{A}_3(1,1) = \frac{-4\xi\rho^3 + (-14+24\xi^2)\rho^2 + 48\xi\rho + 36}{\rho^4 + 8\xi\rho^3 + (4+24\xi^2)\rho^2 + 48\xi\rho + 36}, \tag{22a}$$

$$\mathbf{A}_3(1,2) = \frac{(-2\rho^3 + 12\xi\rho^2 + 36\rho)/\omega}{\rho^4 + 8\xi\rho^3 + (4+24\xi^2)\rho^2 + 48\xi\rho + 36}, \tag{22b}$$

$$\mathbf{A}_3(2,1) = \frac{(2\rho^3 - 12\xi\rho^2 - 36\rho)\omega}{\rho^4 + 8\xi\rho^3 + (4+24\xi^2)\rho^2 + 48\xi\rho + 36}, \tag{22c}$$

$$\mathbf{A}_3(2,2) = \frac{-14\rho^2 - 24\xi\rho + 36}{\rho^4 + 8\xi\rho^3 + (4+24\xi^2)\rho^2 + 48\xi\rho + 36}, \tag{22d}$$

where $\rho = \omega\Delta t$. It can be shown that equation (22) is equivalent to the first sub-diagonal (1, 2) Padé approximation. Hence, the first sub-diagonal (1, 2) Padé approximation is

re-derived by the present complex-time-step Newmark methods. The algorithm is asymptotic annihilating, unconditionally stable (hence L-stable) and third order accurate.

7.2. FOURTH ORDER NON-DISSIPATIVE A-STABLE ALGORITHM

Consider the non-dissipative algorithm with $\mu = 1$. The algorithmic parameters in equation (13) are

$$\alpha_0 = 1, \qquad \alpha_1 = i\sqrt{3}, \qquad \alpha_2 = -i\sqrt{3}, \qquad \beta_0 = 0, \qquad \beta_1 = \frac{1}{2} - i\frac{\sqrt{3}}{6}, \qquad \beta_2 = \frac{1}{2} + i\frac{\sqrt{3}}{6}, \tag{23}$$

and the entries of the numerical amplification in equation (20) are

$$\mathbf{A}_4(1,1) = \frac{\rho^4 - 12\xi\rho^3 + (-60 + 48\xi^2)\rho^2 + 144\xi\rho + 144}{\rho^4 + 12\xi\rho^3 + (12 + 48\xi^2)\rho^2 + 144\xi\rho + 144}, \tag{24a}$$

$$\mathbf{A}_4(1,2) = \frac{(-12\rho^3 + 144\rho)/\omega}{\rho^4 + 12\xi\rho^3 + (12 + 48\xi^2)\rho^2 + 144\xi\rho + 144}, \tag{24b}$$

$$\mathbf{A}_4(2,1) = \frac{(12\rho^3 - 144\rho)\omega}{\rho^4 + 12\xi\rho^3 + (12 + 48\xi^2)\rho^2 + 144\xi\rho + 144}, \tag{24c}$$

$$\mathbf{A}_4(2,2) = \frac{\rho^4 + 12\xi\rho^3 + (-60 + 48\xi^2)\rho^2 - 144\xi\rho + 144}{\rho^4 + 12\xi\rho^3 + (12 + 48\xi^2)\rho^2 + 144\xi\rho + 144}, \tag{24d}$$

where $\rho = \omega\Delta t$. It can be shown that equation (24) is equivalent to the diagonal (2, 2) Padé approximation. Hence, the diagonal (2, 2) Padé approximation is re-derived by the present complex-time-step Newmark methods. The algorithm is non-dissipative, unconditionally stable and fourth order accurate.

7.3. COMPUTATIONAL EFFORT

Since complex numbers are used in the evaluation, the computational effort is higher than normal real numbers calculation. In general, the effort for complex number multiplication is four times higher than that of real number multiplication. However, it can be seen that β_1 and β_2 are complex conjugates. The numerical results corresponding to β_2 can be obtained from β_1 directly since

$$\alpha_2[\mathbf{A}_{NM}(\beta_2\,\Delta t)] = \bar{\alpha}_1[\mathbf{A}_{NM}(\bar{\beta}_1\,\Delta t)] = \overline{\alpha_1[\mathbf{A}_{NM}(\beta_1\,\Delta t)]}. \tag{25}$$

As a result, the present third order complex-time-step algorithms require four times the effort of an ordinary Newmark method to advance one time step. However, the present algorithms have the advantages of being third order accurate, unconditionally stable with controllable numerical dissipation, while the Newmark method is only second order accurate, unconditionally stable and non-dissipative if $2\beta \geqslant \gamma = 1/2$ or first order accurate, unconditionally stable and dissipative if $2\beta \geqslant \gamma > 1/2$.

For Tarnow and Simo's method, it can be seen that the computational effort is roughly three times that of the Newmark method as there are three evaluations to advance one time step. However, as shown later on, the method is not very accurate although it is a fourth order algorithm. The fourth order extrapolation Newmark method requires three evaluations as well. However, the method is unconditionally unstable. When the third order accurate L-stable (1, 2) Padé approximation and the fourth order accurate A-stable (2, 2) Padé approximation are expressed in matrix form [6, 10], the bandwidth and the matrix size are doubled. The computational effort is therefore increased by four times.

TABLE 1

Parameters for the fifth order complex-time-step Newmark methods

μ	β_0	β_1	Re (β_2)	Im (β_2)	Re (β_3)	Im (β_3)
1·0	0	0·430629	0·284686	0·271600	0·284686	−0·271600
0·9	0	0·439978	0·285274	0·279493	0·285274	−0·279493
0·8	0	0·449535	0·286344	0·287727	0·286344	−0·287727
0·7	0	0·459389	0·287952	0·296333	0·287952	−0·296333
0·6	0	0·469644	0·290178	0·305346	0·290178	−0·305346
0·5	0	0·480424	0·293121	0·314804	0·293121	−0·314804
0·4	0	0·491885	0·296915	0·324747	0·296915	−0·324747
0·3	0	0·504226	0·301733	0·335210	0·301733	−0·335210
0·2	0	0·517714	0·307809	0·346225	0·307809	−0·346225
0·1	0	0·532719	0·315458	0·357800	0·315458	−0·357800
0·0	0	0·549778	0·325111	0·369899	0·325111	−0·369899
μ	α_0	α_1	Re (α_2)	Im (α_2)	Re (α_3)	Im (α_3)
1·0	0·00	6·158266	−2·579133	0·337708	−2·579133	−0·337708
0·9	0·05	5·693062	−2·371531	0·271472	−2·371531	−0·271472
0·8	0·10	5·260683	−2·180341	0·201943	−2·180341	−0·201943
0·7	0·15	4·856633	−2·003316	0·130540	−2·003316	−0·130540
0·6	0·20	4·476854	−1·838427	0·058274	−1·838427	−0·058274
0·5	0·25	4·117655	−1·683827	−0·014149	−1·683827	0·014149
0·4	0·30	3·775628	−1·537814	−0·086257	−1·537814	0·086257
0·3	0·35	3·447553	−1·398776	−0·157763	−1·398776	0·157763
0·2	0·40	3·130276	−1·265138	−0·228542	−1·265138	0·228542
0·1	0·45	2·820562	−1·135281	−0·298631	−1·135281	0·298631
0·0	0·50	2·514889	−1·007444	−0·368254	−1·007444	0·368254

This is comparable to the present method. However, the present method is more general as the numerical dissipation is controllable.

8. OTHER HIGHER ORDER ALGORITHMS

8.1. FIFTH ORDER ALGORITHMS

Using an additional pair of algorithmic parameters, two more equations can be solved. The resultant algorithms would be at least fifth order accurate. It can be shown that β_1, β_2 and β_3 are given by the roots of the following equation for any desirable ultimate spectral radius μ

$$15(1+\mu)x^3 - 6(3+2\mu)x^2 + 3(3+\mu)x - 2 = 0. \tag{26}$$

The corresponding α_0, α_1, α_2 and α_3 can be solved from equations (9a–d). In particular, α_0 is found to be

$$\alpha_0 = (1-\mu)/2. \tag{27}$$

The explicit formulae for α_i and β_i are complicated and are not shown here. Table 1 lists the values of α_i and β_i for μ varying from 0 to 1 by 0·1. The numerical amplification matrix $[\mathbf{A}_5(\Delta t)]$ can be written as

$$\begin{aligned}[\mathbf{A}_5(\Delta t)] &= \alpha_0[\mathbf{I}] + \alpha_1[\mathbf{A}_{NM}(\beta_1\Delta t)] + \alpha_2[\mathbf{A}_{NM}(\beta_2\Delta t)] + \alpha_3[\mathbf{A}_{NM}(\beta_3\Delta t)] \\ &= \alpha_0[\mathbf{I}] + \alpha_1[\mathbf{A}_{NM}(\beta_1\Delta t)] + \alpha_2[\mathbf{A}_{NM}(\beta_2\Delta t)] + \overline{\alpha_2[\mathbf{A}_{NM}(\beta_2\Delta t)]}.\end{aligned} \tag{28}$$

It can be shown that the eigenvalues of the undamped numerical amplification matrix (i.e., with $\xi = 0$) are complex conjugates and the squares of the moduli of the eigenvalues are

$$|\lambda_1|^2 = |\lambda_2|^2 = \det([\mathbf{A}_5])$$
$$= 1 - \frac{\omega^6 \Delta t^6 (1-\mu^2)}{\omega^6 \Delta t^6 + 3(3+2\mu+3\mu^2)\omega^4 \Delta t^4 + 4(54+72\mu+54\mu^2)\omega^2 \Delta t^2 + 3600(1+\mu)^2}. \tag{29}$$

It can be shown that $\det([\mathbf{A}_5]) \geqslant 0$ for all real values of $\omega\Delta t$ and μ. Also, the algorithm is conditionally stable with the spectral radius exceeding unity for some values of $\omega\Delta t$ if $\mu > 1$ or $\mu < -1$. When μ approaches -1, some of the algorithmic parameters are undefined and the formulation is not valid. As a result, the algorithm is unconditionally C-stable only when $1 \geqslant \mu > -1$. Besides, it can be seen that the spectral radius monotonically decreases as $\omega\Delta t$ increases. This gives good algorithmic damping properties as the high-frequency responses are damped out progressively.

The leading truncation error terms for the entries in $[\mathbf{A}_5]$–$[\mathbf{A}]$ can be shown to be proportional to

$$\Sigma \alpha_i \beta_i^6 - 2/45 = \frac{(1-\mu)}{225(1+\mu)}. \tag{30}$$

It can be shown that the relative period error and algorithmic damping ratio for the fifth order accurate algorithm are

$$\text{Relative period error} = \frac{3\mu^2 - \mu + 3}{126000(1+2\mu+\mu^2)}\,\omega^6 \Delta t^6 + O(\Delta t^8), \tag{31a}$$

$$\text{Algorithmic damping ratio} = \frac{(1-\mu)}{7200(1+\mu)}\,\omega^5 \Delta t^5 + O(\Delta t^7). \tag{31b}$$

It can be shown that if $\mu = -1$, the formulation is not valid as some of the parameters are undefined. The leading error term in equation (31a) is minimized when $\mu = 1$. In this case, the algorithm is non-dissipative and sixth order accurate.

It can be shown that the spectral radius is less than unity for $1 > \mu > -1$. Besides, it can be seen that the errors increase as μ decreases from 1. As a result, for a desirable ultimate spectral radius $|\lambda_\infty|$, $\mu = |\lambda_\infty|$ would give better results than $\mu = -|\lambda_\infty|$. In conclusion, only algorithms with $0 \leqslant \mu \leqslant 1$ would be useful.

It can be shown that the algorithms corresponding to $\mu = 0$ and $\mu = 1$ are the first sub-diagonal (2, 3) and diagonal (3, 3) Padé approximations respectively.

8.2. SEVENTH ORDER ALGORITHMS

Using an additional pair of algorithmic parameters, two more equations can be solved. The resultant algorithms are at least seventh order accurate. It can be shown that β_1, β_2, β_3 and β_4 are given by the roots of the following equation for any desirable ultimate spectral radius μ

$$105(1+\mu)x^4 - 30(4+3\mu)x^3 + 30(2+\mu)x^2 - 4(4+\mu)x + 2 = 0. \tag{32}$$

The corresponding α_0, α_1, α_2, α_3 and α_4 can be solved from equations (9a–e). In particular, α_0 is found to be

$$\alpha_0 = (1+\mu)/2. \tag{33}$$

The explicit formulae for α_i and β_i are complicated and are not shown here. Table 2 lists the values of α_i and β_i for μ from 0 to 1 by 0·1. The numerical amplification matrix $[\mathbf{A}_7(\Delta t)]$ can be written as

$$\begin{aligned}[\mathbf{A}_7(\Delta t)] &= \alpha_0[\mathbf{I}] + \alpha_1[\mathbf{A}_{NM}(\beta_1\Delta t)] + \alpha_2[\mathbf{A}_{NM}(\beta_2\Delta t)] + \alpha_3[\mathbf{A}_{NM}(\beta_3\Delta t)] + \alpha_4[\mathbf{A}_{NM}(\beta_4\Delta t)] \\ &= \alpha_0[\mathbf{I}] + \alpha_1[\mathbf{A}_{NM}(\beta_1\Delta t)] + \overline{\alpha_1[\mathbf{A}_{NM}(\beta_1\Delta t)]} + \alpha_3[\mathbf{A}_{NM}(\beta_3\Delta t)] \\ &\quad + \overline{\alpha_3[\mathbf{A}_{NM}(\beta_3\Delta t)]}. \end{aligned} \tag{34}$$

It can be shown that the eigenvalues of the undamped numerical amplification matrix (i.e., with $\xi = 0$) are complex conjugates and the squares of the moduli of the eigenvalues are

$$|\lambda_1|^2 = |\lambda_2|^2 = \det([\mathbf{A}_7]) = 1 - \frac{\omega^8\Delta t^8(1-\mu^2)}{\omega^8\Delta t^8 + 8(2+\mu+2\mu^2)\omega^6\Delta t^6 + 720(1+\mu+\mu^2)\omega^4\Delta t^4 \cdot \\ +14400(2+3\mu+2\mu^2)\omega^2\Delta t^2 + 705600(1+\mu)^2}. \tag{35}$$

It can be shown that $\det([\mathbf{A}_7]) \geqslant 0$ for all real values of $\omega\Delta t$ and μ. Also, the algorithm is conditionally stable with the spectral radius exceeding unity for some values of $\omega\Delta t$ if $\mu > 1$ or $\mu < -1$. When μ approaches -1, some of the algorithmic parameters are undefined and the formulation is not valid. As a result, the algorithm is unconditionally C-stable only when $1 \geqslant \mu > -1$. Besides, it can be seen that the spectral radius monotonically decreases as $\omega\Delta t$ increases. This gives good algorithmic damping properties as the high-frequency responses are damped out progressively.

The leading truncation error terms for the entries in $[\mathbf{A}_7]$–$[\mathbf{A}]$ can be shown to be proportional to

$$\Sigma\alpha_i\beta_i^8 - 1/315 = -\frac{(1-\mu)}{11025(1+\mu)}. \tag{36}$$

It can be shown that the relative period error and algorithmic damping ratio for the seventh order accurate algorithm are

$$\text{Relative period error} = \frac{4\mu^2 - \mu + 4}{44452800(1+2\mu+\mu^2)}\omega^8\Delta t^8 + O(\Delta t^{10}), \tag{37a}$$

$$\text{Algorithmic damping ratio} = \frac{(1-\mu)}{1411200(1+\mu)}\omega^7\Delta t^7 + O(\Delta t^9). \tag{37b}$$

It can be shown that if $\mu = -1$, the formulation is not valid as some of the parameters are undefined. The leading error term in equation (37a) is minimized when $\mu = 1$. In this case, the algorithm is non-dissipative and eighth order accurate.

It can be shown that the spectral radius is less than unity for $1 > \mu > -1$. Besides, it can be seen that the errors increase as μ decreases from 1. As a result, for a desirable ultimate spectral radius $|\lambda_\infty|$, $\mu = |\lambda_\infty|$ would give better results than $\mu = -|\lambda_\infty|$. In conclusion, only algorithms with $0 \leqslant \mu \leqslant 1$ would be useful.

It can be shown that the algorithms corresponding to $\mu = 0$ and $\mu = 1$ are the first sub-diagonal (3, 4) and diagonal (4, 4) Padé approximations respectively.

9. COMPARISON WITH OTHER ALGORITHMS

The spectral radii for various algorithms are shown in Figure 2(a). The notations used are shown in Table 3. It can be seen that both the Houbolt and Park methods are asymptotic annihilating. However, the dissipation in the low-frequency range is quite

TABLE 2

Parameters for the seventh order complex-time-step Newmark methods

μ	β_0	Re (β_1)	Im (β_1)	Re (β_2)	Im (β_2)	Re (β_3)	Im (β_3)	Re (β_4)	Im (β_4)
1·0	0	0·183132	−0·231325	0·183132	0·231325	0·316868	−0·094882	0·316868	0·094882
0·9	0	0·182263	−0·235693	0·182263	0·235693	0·321497	−0·097836	0·321497	0·097836
0·8	0	0·181671	−0·240328	0·181671	0·240328	0·326266	−0·100704	0·326266	0·100704
0·7	0	0·181391	−0·245242	0·181391	0·245242	0·331214	−0·103515	0·331214	0·103515
0·6	0	0·181468	−0·250448	0·181468	0·250448	0·336389	−0·106292	0·336389	0·106292
0·5	0	0·181958	−0·255958	0·181958	0·225958	0·341851	−0·109060	0·341851	0·109060
0·4	0	0·182934	−0·261789	0·182934	0·261789	0·347678	−0·111843	0·347678	0·111843
0·3	0	0·184490	−0·267950	0·184490	0·267950	0·353971	−0·114664	0·353971	0·114664
0·2	0	0·186752	−0·274447	0·186752	0·274447	0·360867	−0·117544	0·360867	0·117544
0·1	0	0·189882	−0·281267	0·189882	0·281267	0·368559	−0·120502	0·368559	0·120502
0·0	0	0·194101	−0·288365	0·194101	0·288365	0·377328	−0·123549	0·377328	0·123549
μ	α_0	Re (α_1)	Im (α_1)	Re (α_2)	Im (α_2)	Re (α_3)	Im (α_3)	Re (α_4)	Im (α_4)
1·0	1·00	1·143875	−3·452041	1·143875	3·452041	−1·1438746	15·298158	−1·143875	−15·298158
0·9	0·95	0·996028	−3·166311	0·996028	3·166311	−0·9710284	14·073755	−0·971028	−14·073755
0·8	0·90	0·842873	−2·907528	0·842873	2·907528	−0·7928726	12·951998	−0·792873	−12·951998
0·7	0·85	0·687594	−2·672203	0·687594	2·672203	−0·6125939	11·916337	−0·612594	−11·916337
0·6	0·80	0·532419	−2·456956	0·532419	2·456956	−0·4324191	10·952723	−0·432419	−10·952723
0·5	0·75	0·378821	−2·258594	0·378821	2·258594	−0·2538207	10·049014	−0·253821	−10·049014
0·4	0·70	0·227678	−2·074122	0·227678	2·074122	−0·0776776	9·194480	−0·077678	−9·194480
0·3	0·65	0·079387	−1·900719	0·079387	1·900719	0·09561291	8·379353	0·095613	−8·379353
0·2	0·60	−0·066071	−1·735681	−0·066071	1·735681	0·26607113	7·594395	0·266071	−7·594395
0·1	0·55	−0·209127	−1·576336	−0·209127	1·576336	0·43412707	6·830393	0·434127	−6·830393
0·0	0·50	−0·350689	−1·419933	−0·350689	1·419933	0·60068857	6·077528	0·600689	−6·077528

severe for the Houbolt method. The (1, 2) Padé approximation is asymptotic annihilating with much smaller low-frequency dissipation. This algorithm is equivalent to the present third order complex-time-step algorithm with $\mu = 0$. For other values of μ, the spectral radii are decreasing smoothly to the respective ultimate spectral radii. The present complex-time-step algorithm is non-dissipative when $\mu = 1$.

Figure 3(a) shows the spectral radii for various high order complex-time-step algorithms. The same trend can be observed as the third order algorithms. The spectral radii are decreasing smoothly to the respective ultimate spectral radii. The higher order algorithms exhibit smaller low-frequency dissipation, as expected.

The extrapolated Newmark method evaluates the results at the end of the time step several times with different sub-step sizes. The numerical results given by the extrapolated Newmark methods are very accurate. Unfortunately, the extrapolated Newmark methods are unconditionally unstable. The spectral radii for the fourth, sixth and eighth order extrapolated Newmark method (denoted as ENM4, ENM6 and ENM8 respectively) are shown in Figure 4 for comparison.

Figure 2(b) shows the algorithmic damping ratios for various algorithms. The present third order complex-time-step algorithms are comparable to the second order algorithms. Figure 3(b) shows the algorithmic damping ratios for various higher order complex-time-step algorithms. The algorithms are separated into three groups with increasing accuracy. The algorithmic damping ratios for the extrapolated Newmark methods are also shown in Figure 3(b). However, the values should be negative indicating that they are numerically unstable.

Figure 2(c) shows the relative period errors for various algorithms. It can be seen that the relative period errors for the present third order complex-time-step algorithms are smaller than those for the second order algorithms. The relative period errors of the present third order algorithms are better than Tarnow and Simo's fourth order algorithm (TSNM). Figure 3(c) shows the relative period errors for various higher order complex-time-step algorithms. It can be seen that the relative period errors for the fourth,

TABLE 3

Notations for various algorithms

Method	Notation
Houbolt	Houbolt
Park	Park
HHT ($\alpha = -0{\cdot}3$)	HHT
Newmark ($\beta = 1/4, \gamma = 1/2$)	NM
Central difference ($\beta = 0, \gamma = 1/2$)	CD
Fox–Goodwin ($\beta = 1/12, \gamma = 1/2$)	FG
Extrapolated Newmark	ENM4
Extrapolated Newmark	ENM6
Extrapolated Newmark	ENM8
Tarrow and Simo's Newmark	TSNM
(1, 2) Padé approximation	P12
(2, 2) Padé approximation	P22
Present: third order	CTS3
Present: fourth order	CTS4
Present: fifth order	CTS5
Present: sixth order	CTS6
Present: seventh order	CTS7
Present: eighth order	CTS8

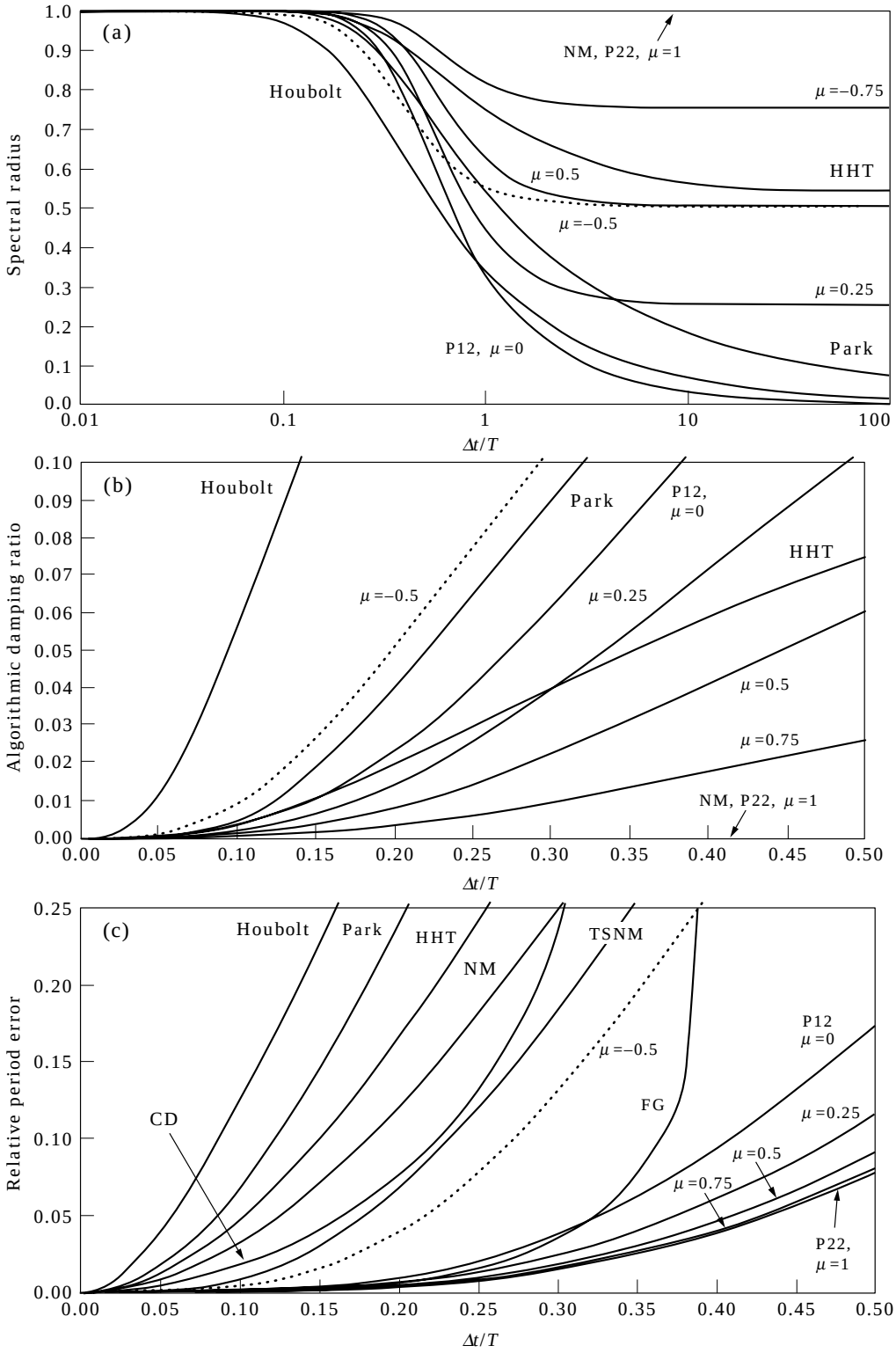

Figure 2. (a) Comparison of spectral radii with third order complex-time-step algorithms ($\xi = 0$). (b) Comparison of algorithmic damping ratios with third order complex-time-step algorithms ($\xi = 0$). (c) Comparison of relative period errors with third order complex-time-step algorithms ($\xi = 0$).

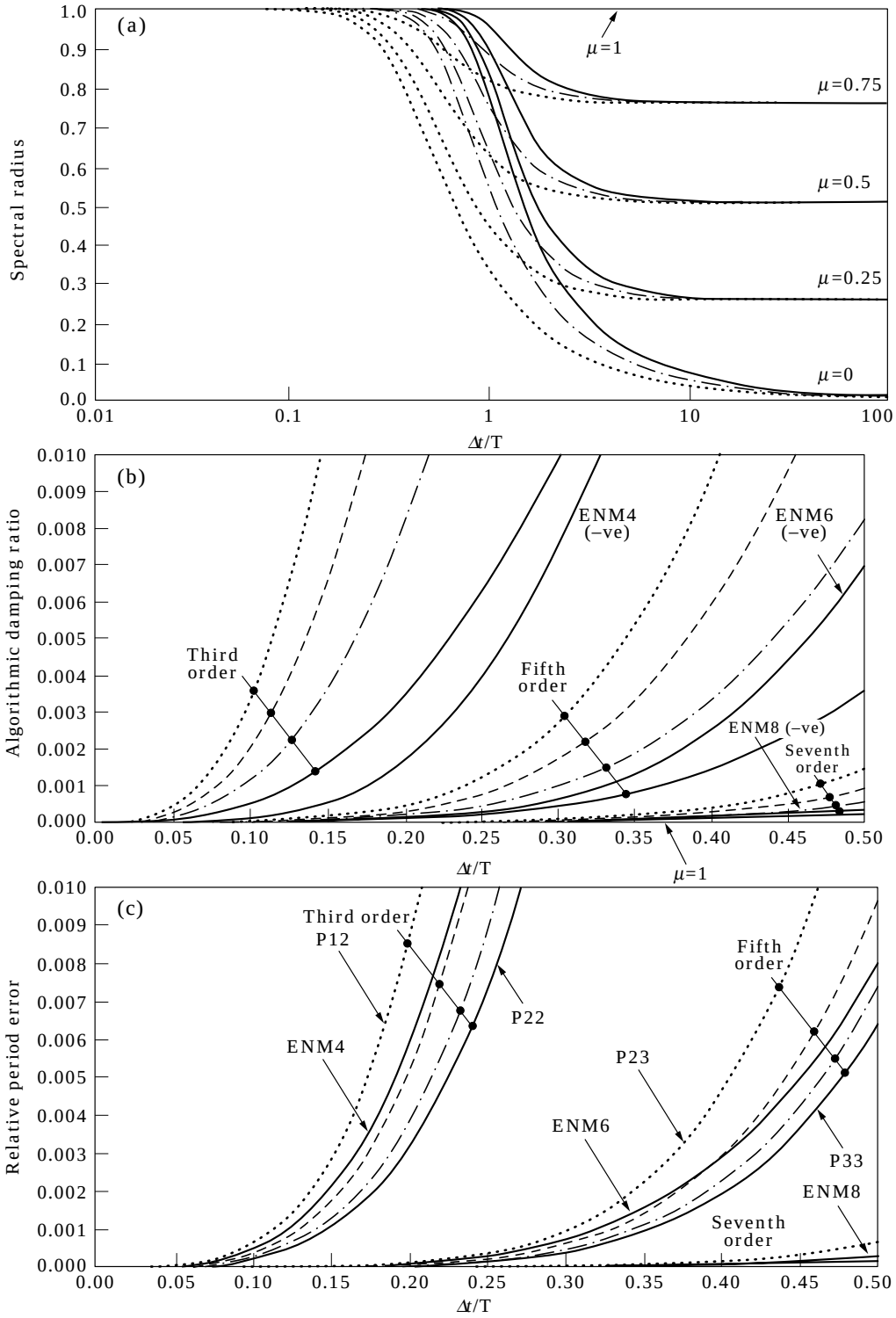

Figure 3. (a) Comparison of spectral radii with various higher order complex-time-step algorithms ($\xi = 0$); - - - - -, third order; – · – · , fifth order; ——, seventh order. (b) Comparison of algorithmic damping ratios with various higher order complex-time-step algorithms ($\xi = 0$); · · · · · $\mu = 0$; – – –, $\mu = 0{\cdot}25$; – · – ·, $\mu = 0{\cdot}5$; ——, $\mu = 0{\cdot}75$. (c) Comparison of relative period errors with various higher order complex-time-step algorithms ($\xi = 0$); · · · ·, $\mu = 0$; – – –, $\mu = 0{\cdot}25$; – · –, $\mu = 0{\cdot}5$; ——, $\mu = 1$.

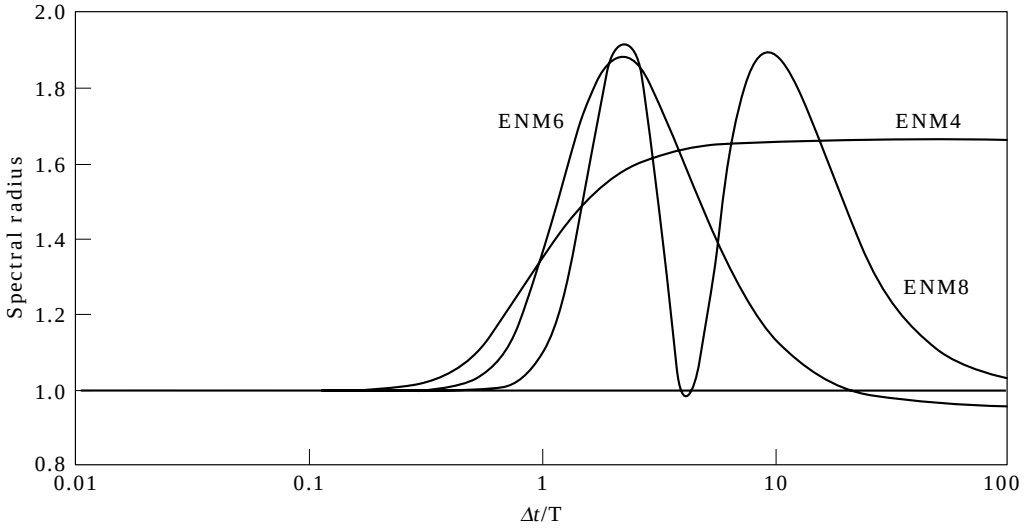

Figure 4. Spectral radii for the extrapolated Newmark methods ($\xi = 0$).

sixth and eighth order extrapolated Newmark algorithms are comparable to the present third, fifth and seventh order algorithms. However, the extrapolated Newmark methods are unconditionally unstable.

In Figures 2(a–c), the spectral radii, the algorithmic damping ratios and the relative period errors for the third order complex-time-step algorithm with $\mu = -0{\cdot}5$ are shown. The algorithm has the same ultimate spectral radius as $\mu = 0{\cdot}5$. It can be seen that the algorithm is not as accurate as the algorithm with $\mu = 0{\cdot}5$. This is also true for other values of $|\mu|$ for other higher order complex-time-step algorithms. As a result, only $0 \leqslant \mu \leqslant 1$ gives useful algorithms.

10. NUMERICAL EXAMPLE

Consider a single-degree-of-freedom system governed by

$$\ddot{u}(t) + 2\xi\omega\dot{u}(t) + \omega^2 u(t) = f(t), \tag{38}$$

where $\xi = 0$, $\omega = 1$ and $f(t) = 0$. The initial conditions are $u_0 = 1$ and $v_0 = 0$. The period of the system is 2π. A time-step size of about one-tenth of the period of the system is usually recommended for second order accurate algorithms. Figures 5(a and b) show the calculated results by various methods with different time-step sizes. The algorithms are denoted by the notations shown in Table 3, with an additional digit appended to indicate the time-step size used. For example, CTS41 indicates the present fourth order complex-time-step algorithm with $\Delta t = 1$.

Figure 5(a) shows the numerical results of the ordinary second order Newmark method with $\Delta t = 0{\cdot}25$ (NM0·25) and $\Delta t = 0{\cdot}5$ (NM0·5). The results with $\Delta t = 0{\cdot}25$ are acceptable while the results with $\Delta t = 0{\cdot}5$ are not very good. Although Tarnow and Simo's Newmark method is fourth order accurate, it can be seen from Figure 5(a) that the results with $\Delta t = 1$ are not accurate. On the other hand, the fourth order extrapolated Newmark method and the present fourth order complex-time-step method give accurate results with $\Delta t = 1$.

Figure 5(b) shows the numerical results of the higher order algorithms with $\Delta t = 2$ and 4. It can be seen that Tarnow and Simo's Newmark method with $\Delta t = 2$ is not accurate. The present fourth order complex-time-step algorithm gives better results than the fourth order extrapolated Newmark method when $\Delta t = 2$. The sixth order extrapolated Newmark method and the present sixth order complex-time-step method give good results when $\Delta t = 2$. The eighth order algorithms still give good results when $\Delta t = 4$! The accuracy of higher order algorithms is clearly demonstrated.

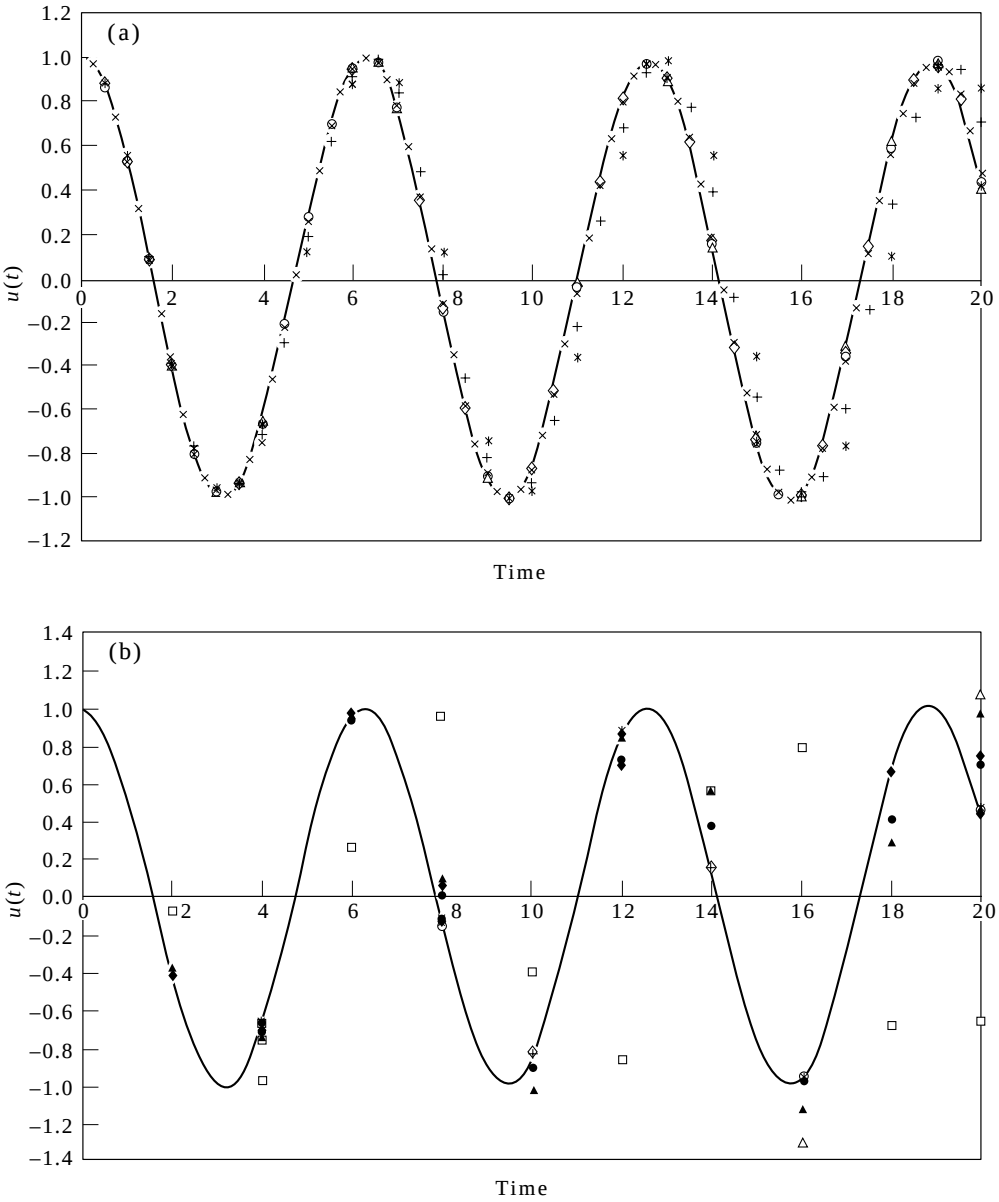

Figure 5. (a) Results for the numerical example with $\Delta t \leqslant 1$; ——, exact; ×, NM0·25; +, NM0·5; ◇, TSNM0·5; ∗, TSNM1; ○, ENM41; △, CTS41. (b) Results for the numerical example with $\Delta t \geqslant 2$; ——, exact; □, TSNM2; ▲, ENM42; +, ENM62; △, ENM64; ∗, ENM84; ●, CTS42; ◇, CTS62; ◆, CTS64; ○, CTS84.

Note that the extrapolated Newmark methods are numerically unstable although the numerical results are very accurate. The numerical results would eventually diverge.

11. CONCLUSIONS

Unconditionally stable higher order time-step integration algorithms are presented. To advance one time step, the numerical results at a few sub-step locations are calculated and combined linearly. The sub-step locations are expressed in terms of complex number. The weighting factors and the sub-step locations are algorithmic parameters. The parameters are determined to eliminate the leading truncation error terms. The parameters are expressed in terms of the ultimate spectral radius. As a result, higher order accurate unconditionally stable algorithms with any desirable high-frequency dissipation can be constructed easily. It is shown that the algorithms are unconditionally stable if the ultimate spectral radius is less than unity. The spectral radii of the algorithms are found decreasing gradually toward the design ultimate spectral radii as the time-step size increases without any cusps. Besides, the eigenvalues for the numerical amplification matrix are complex conjugates. The algorithms are all C-stable. Among all the algorithms, the asymptotic annihilating algorithm and non-dissipative algorithm are found to be the first sub-diagonal and diagonal Padé approximations respectively. The stability properties and errors for the present algorithms with other ultimate spectral radii are between these two algorithms. The third order algorithms are derived in detail. The algorithmic parameters for the fifth and seventh order algorithms are given explicitly. When the algorithms are non-dissipative, the order of accuracy is increased by one.

The spectral radii, the algorithmic damping ratios and the relative period errors for the present higher order complex-time-step algorithms and other higher order algorithms are presented. The present algorithms have the advantages of low computational effort, with controllable dissipation and are suitable for parallel implementation.

REFERENCES

1. W. L. Wood 1990 *Practical Time-stepping Schemes*. Oxford: Clarendon Press.
2. T. J. R. Hughes 1987 *The Finite Element Method: Linear Static and Dynamic Finite Element Analysis*. Englewood Cliffs, NJ: Prentice-Hall.
3. O. C. Zienkiewicz and R. L. Taylor 1991 *The Finite Element Method*. New York: McGraw-Hill: fourth edition.
4. E. Hairer, S. P. Nørestt and G. Wanner 1987 *Solving Ordinary Differential Equations I*. Berlin: Springer.
5. E. Hairer and G. Wanner 1991 *Solving Ordinary Differential Equations II*. Berlin: Springer.
6. P. W. Möller 1993 *International Journal for Numerical Methods in Engineering* **36**, 2607–2624. High-order hierarchical A- and L-stable integration methods.
7. M. Borri and C. Bottasso 1993 *Computational Mechanics* **13**, 133–142. A general framework for interpreting time finite element formulations.
8. G. M. Hulbert 1992 *International Journal for Numerical Methods in Engineering* **33**, 307–331. Time finite element methods for structural dynamics.
9. G. M. Hulbert 1994 *Computer Methods in Applied Mechanics and Engineering* **113**, 1–9. A unified set of single-step asymptotic annihilation algorithms for structural dynamics.
10. T. C. Fung 1996 *International Journal for Numerical Methods in Engineering* **39**, 3475–3495. Unconditionally stable higher order accurate Hermitian time finite elements.
11. M. Austin 1993 *International Journal for Numerical Methods in Engineering* **36**, 2107–2122. Higher order integration of smooth dynamical systems: theory and numerical experiments.
12. W. X. Zhong and F. W. Williams 1994 *Journal of Mechanical Engineering Science*, *Proceedings of the Institute of the Mechanical Engineers*, *Part C* **208**, 427–430. A precise time step integration method.

13. J. H. Lin, W. P. Shen and F. W. Williams 1995 *Computers and Structures* **56**, 113–120. A high precision direct integration scheme for structures subjected to transient dynamic loading.
14. W. X. Zhong, J. N. Zhu and X. X. Zhong 1996 *Computer Methods in Applied Mechanics and Engineering* **130**, 163–178. On a new time integration method for solving time dependent partial differential equations.
15. T. C. Fung, *International Journal for Numerical Methods in Engineering*. A precise time-step integration method by step-response and impulsive-response matrices for dynamic problems. In press.
16. N. Tarnow and J. C. Simo 1994 *Computer Methods in Applied Mechanics and Engineering* **115**, 233–252. How to render second order accurate time-stepping algorithms fourth order accurate while retaining the stability and conservation properties.